We are IntechOpen,
the world's leading publisher of
Open Access books
Built by scientists, for scientists

4,900
Open access books available

124,000
International authors and editors

140M
Downloads

Our authors are among the

154
Countries delivered to

TOP 1%
most cited scientists

12.2%
Contributors from top 500 universities

BOOK CITATION INDEX
CLARIVATE ANALYTICS
INDEXED

WEB OF SCIENCE™

Selection of our books indexed in the Book Citation Index
in Web of Science™ Core Collection (BKCI)

Interested in publishing with us?
Contact book.department@intechopen.com

Numbers displayed above are based on latest data collected.
For more information visit www.intechopen.com

Synthesis of Planar EBG Structures Based on Genetic Programming

Luisa Deias, Giuseppe Mazzarella and Nicola Sirena
University of Cagliari
Italy

1. Introduction

1.1 Electronic Band–Gap (EBG) structures

Frequency selective surfaces (FSS) consist of two-dimensional periodic arrays of metal patches patterned on a dielectric substrate or apertures etched on a metal screen (Hosseini et al., 2006; Wu, 1995; Yang et al., 1999).

These periodic structures resonate at certain frequencies, thus ensuring filtering characteristics, exploited both in the microwave and optical region of the electromagnetic spectrum. Frequency selective surfaces have been thoroughly studied over the years (Mittra et al., 1988; Munk, 2000), and they have found new life in the past decade when *electromagnetic bandgap* (EBG) (Sievenpiper et al., 1999; Yang et al., 1999) structures were introduced, firstly under the name of photonic bandgap (PBG) materials, in analogy to the bandgaps present in electric crystals, even though no photons were involved. Some well–known EBG structures are the Uniplanar Compact Photonic Band-Gap (UC–PBG)(Yang et al., 1999) (Fig. 1) and the Sievenpiper "mushroom" high–impedance surface (Sievenpiper et al., 1999).
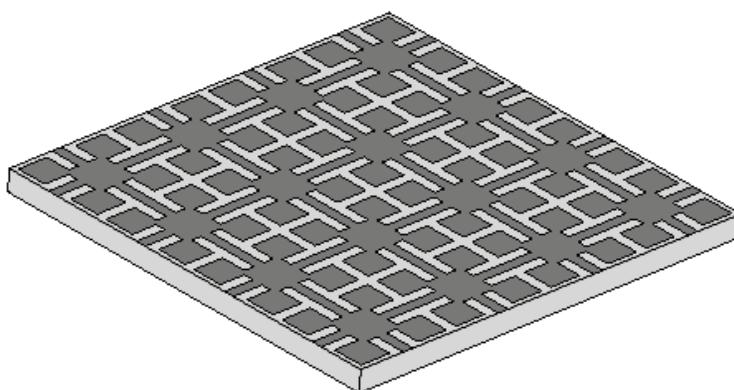

Fig. 1. Uniplanar Compact Photonic Band-Gap (UC–PBG)(Yang et al., 1999)

This entirely new class of structures, encompassing FSS as one of its subclasses (planar EBG) display some very interesting new electromagnetic properties. The presence of a stopband for this structure has been theoretically and experimentally verified and exploited

in different realizations, i.e. TEM waveguide, slow–wave planar structure and low–loss conductor–backed coplanar waveguide.

By choosing the proper geometry of the periodic surface we can shape the electromagnetic behavior of these structures and they can be made to act as a so–called electromagnetic crystal, exhibiting frequency bands inside which the propagation of electromagnetic waves is not allowed or is highly attenuated. The concept of suppressing surfaces waves on metals is not new. Surface waves can be eliminated from a metal surface over a finite frequency band by applying a periodic texture. It has been done long before EGB structures were introduced using several geometries, such as a metal sheet covered with small bumps or a corrugated metal slab.

The novelty of EBGs is the application of an array of periodic patches or apertures, i.e. lumped circuit elements, to produce a thin two–dimensional structure that must generally be described by band structure concepts, even though the thickness and periodicity are both much smaller than the operating wavelength.

These periodic structures can also be designed to act as an *artificial magnetic conductor* (AMC) or high–impedance electromagnetic ground plane over a desired (quite) narrow frequency range, corresponding to the forbidden frequency band. Hence, the key feature of these structures is the reflection of an incident plane wave with no phase reversal, unlike normal metal surfaces (Sievenpiper et al., 1999).

High–impedance surfaces are widely studied now as promising antenna substrates (Feresidis et al., 2005; Gonzalo et al., 1999; Hosseini et al., 2006). A possibility of realizing a magnetic wall near the resonant frequency of a very thin structure is very attractive, since this allows one to design low–profile antennas and enhance the performance of printed antennas. The main drawback of this strategy is the reduced bandwidth of the complete antenna, since the frequency range over which these EBG surfaces behave as an AMC is usually narrowband and fixed by their geometrical configuration. The ultimate goal is then to design and incorporate such metamaterial–substrates in antenna structures in order to improve antenna performance.

A key issue in the research field of metamaterials is then represented by the design and optimization of EBG structures. Different techniques have been investigated, among which methods of global optimization such as genetic algorithm and particle swarm optimization (PSO),(Bray et al., 2006; Ge et al., 2007; Kovács et al., 2010; Tavallaee & Rahmat-Samii, 2007; Yeo et al., 2002).

1.2 Genetic programming

Genetic Programming (GP) (Koza, 1992) falls into the larger class of evolutionary computations (Fogel, 2006; Michalewicz, 1992), including genetic algorithms, evolution strategies and evolutionary programming, which can be described as highly parallel probabilistic search algorithms imitating the principles of natural evolution for optimization problems, based on the idea that most real–world problems cannot be handled with binary representations. Such algorithms allow task specific knowledge emerge while solving the problem. Genetic Programming, a variant of genetic algorithms yet with marked differences, is an especially interesting form of computational problem solving.

Genetic Algorithms (GA), already widely used in antenna design (Jones & Joines, 2000; Lohn et al., 2001) and more recently also applied to EBG design and optimization (Bray et al., 2006; Ge et al., 2007; Yeo et al., 2002) iteratively transform populations of mathematical objects (typically fixed–length binary character strings), each with an associated fitness value, into new populations using the Darwinian principle of natural selection.

In GP, unlike GA chromosomes need not be represented by bit-strings and the alteration process includes other "genetic" operators appropriate for the given structure and the given problem. We can say that GA works on the "nucleotide" (i.e. bit) level, in the sense that the antenna or EBG structure is completely defined from the beginning and only a handful of parameters remains to be optimized. The approach proposed by Koza assumes no "a priori" structure. Instead, it builds up the structure of the individuals as the procedure evolves. As a consequence, its solution space has the power of the continuum, while the GA solution space is a discrete one, so it is a very small subspace of the former. The goal of genetic programming is not simply to evolve a bit–string representation of some problem but the computer code that solves that problem.

A fixed–length coding such as GA is rather artificial. As it cannot provide a dynamic variability in length, such a coding often causes considerable redundancy and reduces the efficiency of genetic search. In contrast, GP uses high–level building blocks of variable length. Their size and complexity can change during breeding. Moreover, the typical evolution operators work on actual physical structures rather than on sequences of bits with no intuitive link to the EGB surface shape. The enormous power of this strategy fully allows the exploration of more general shapes.

Getting machines to produce human–like results is the reason for the existence of the fields of artificial intelligence and machine learning. Genetic programming addresses this challenge by providing a method for automatically creating a working computer program from a high–level description of the problem. This is the reason why, unlike Genetic Algorithms, Genetic Programs often deliver elegant human–like solutions not anticipated by the programmer, providing only a minimum amount of pre–supplied human knowledge, analysis and information.

Yet, while allowing to explore and evaluate general configurations, this approach can lead to a severely ill–conditioned synthesis problem. A suitable stabilization is therefore obtained by imposing problem–specific requirements, in our case the periodicity of the the surface elements, which is directly related to the resonant frequency, and the physical parameters, which are not so relevant to the problem. We therefore let then the Genetic Programming strategy evaluate every possible shape in the solution space we delimited.

Representation is a key issue in genetic programming (Koza, 1992) because the representation scheme can severely limit the window through which the system "observes" its world.

Since GP manipulates programs by applying genetic operators, a programming language such as LISP was chosen, since it allows each individual, i.e. computer program, to be manipulated as data. Any LISP S–expression can be depicted as a rooted point-labelled tree with ordered branches, as shown in Fig.2. Therefore in GP each individual is a computer program, described through the set of instructions needed to "build" it, typically implemented in S–expressions.
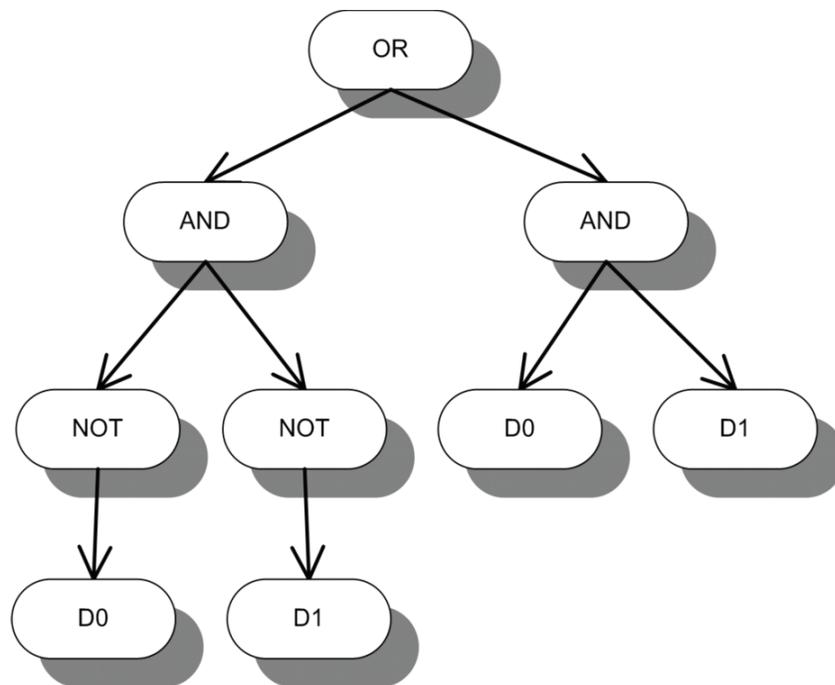
Fig. 2. S-expression: tree architecture.

While the evolutionary "strategy" is almost standard for a variety of problems (we used ECJ, a general purpose Java-based Evolutionary Computation research system and developed at George Mason University ECLab), three elements must be defined to evolve a design, i.e. "individual":

- REPRESENTATION SCHEME:definition of the design space
- VARIATION OPERATORS: code that takes one or more design representations as input and outputs a design derived from them
    - CROSSOVER:creates new S–expressions by exchanging sub S–expressions between two S–expressions. The sub S-expressions exchanged are selected randomly.
    - MUTATION: creates a new S–expression by replacing an existing argument symbol with the other possible symbol. The argument symbol replaced is selected randomly.
- FITNESS FUNCTION: a function that evaluates the individuals

In other words, representation refers to a form of data structure. Variation operations are applied to existing solutions to create new solutions. Usually, variation is based on random perturbation.

The starting point is an initial population of randomly generated computer programs composed of functions and terminals appropriate to the specified problem domain. The evolutionary strategy works in order to find the best individual, in terms of their closeness to the constraints set in the design and evaluated as a "fitness" function. This strategy let to interesting and promising results in the synthesis of EBGs, even when considering more complex structures and requirements (Deias et al., 2009a;b; 2010).

2. EBG design usign genetic programming

In the design of frequency selective surfaces, the choice of the proper element may be of utmost importance. In fact some elements are intrinsically more broad–banded or more narrow–banded than others, while some can be more easily varied by design. In literature we can find a large variety of element types, the more common are illustrated in Fig. 3. It can be now devised the great potential of Genetic Programming, since we don't really want any possible geometry to be taken into account but only feasible geometries, just like a human being would design them on a piece of paper, yet faster and with much more "fantasy".
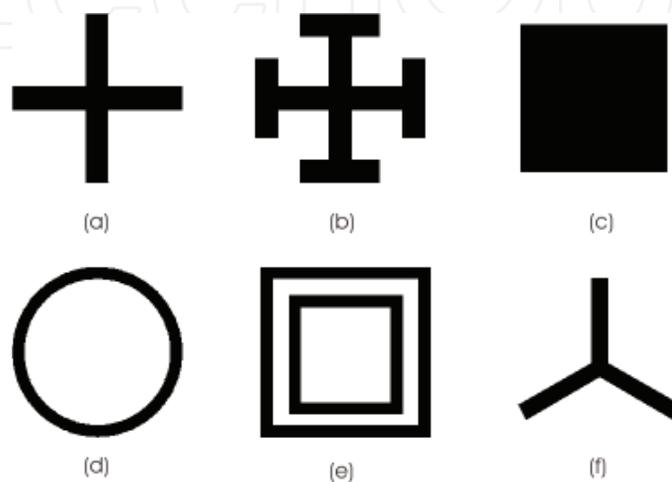
Fig. 3. Some typical FSS unit cell geometries: (a) cross dipole (b) Jerusalem cross (c) square patch (d) circular loop (e) square loops (f) tripole.

Therefore the goal of the design process is to obtain the unit cell aperture geometry of the periodic surface which fulfills the desired requirements on the resonant frequency of the periodic structure, analyzed with a full–wave technique. The GP approach has been implemented in Java, while the full–wave analysis of the periodic structure for each individual has been implemented in Fortran.

The S–expression of an individual of the population can take for example the following form:

```
Tree 0:
 (Branch (Rettangolo 0.16589776 0.2873323
   (Ruota 90.0 (Ruota -90.0 END))) (Ruota 90.0
     (Rettangolo 0.6837649 0.2757175 (Rettangolo 0.7254247 0.23175128
       (Ruota 90.0 (Ruota 90.0 (Ruota -90.0 (Rettangolo 0.19471756 0.19593427
       END)))))))
Tree 1:
 (Branch (Branch END END) (Ruota 90.0 END))
Tree 2:
 (Branch END END)
Tree 3:
 (Ruota 90.0 (Rettangolo 0.51570845 0.25133058
   (Ruota 90.0 (Branch (Ruota -90.0 END) (Rettangolo 0.75231904 0.2833914
   END)))))
```

The corresponding input to the Fortran executable is the following, i.e. a collection of rectangular patches that form the geometry of the aperture:

```
Patch 48
-0.0 , -0.0 , 0.4572 , 0.3048
-0.4572 , -0.0 , 0.4572 , 0.3048
-0.0 , -0.3048 , 0.4572 , 0.3048
-0.4572 , -0.3048 , 0.4572 , 0.3048
-0.3048 , -0.0 , 0.3048 , 0.4572
-0.0 , -0.0 , 0.3048 , 0.4572
-0.3048 , -0.4572 , 0.3048 , 0.4572
-0.0 , -0.4572 , 0.3048 , 0.4572
0.3048 , -0.0 , 0.15239999 , 0.762
-0.4572 , -0.0 , 0.15239999 , 0.762
...
-1.3716 , -0.0 , 0.762 , 0.3048
0.6096 , -0.0 , 0.762 , 0.3048
-0.0 , -0.0 , 0.1524 , 0.3048
-0.1524 , -0.0 , 0.1524 , 0.3048
-0.0 , -0.3048 , 0.1524 , 0.3048
-0.1524 , -0.3048 , 0.1524 , 0.3048
-0.3048 , -0.0 , 0.3048 , 0.1524
-0.0 , -0.0 , 0.3048 , 0.1524
-0.3048 , -0.1524 , 0.3048 , 0.1524
-0.0 , -0.1524 , 0.3048 , 0.1524
```

And the corresponding geometry of the aperture is shown in Fig.4.

Fig. 4. Aperture Geometry.

In our specific problem, we thus obtain a set of rectangular patches which describe the aperture geometry of the EBG unit cell.

The fitness criteria measure the quality of any given solution. The selection method uses the score obtained for each solution to determine which to save and which to eliminate from the population at each generation. Those solutions that survive are the "parents" of the next generation. The initialization of an evolutionary algorithm can be completely at random, or can incorporate human or other expertise about solutions that may work better than others.
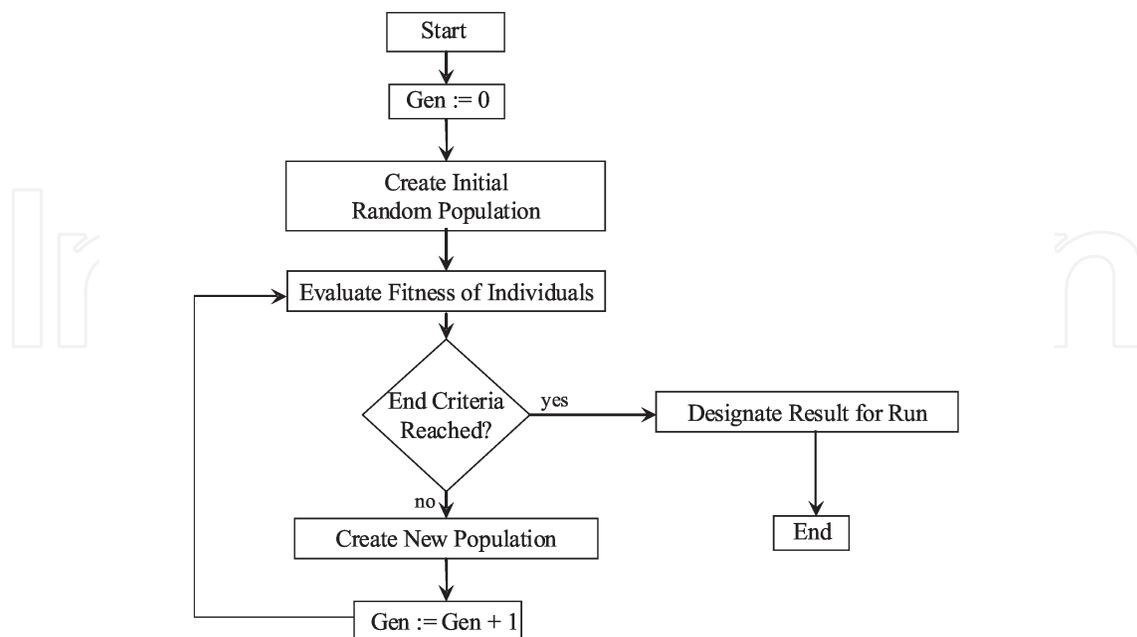
Fig. 5. Flowchart.

The fitness function employed by our GP optimization is:

$$FF = \omega_1 * \omega_2 * e^{\frac{Phase(f_c)}{20}} \tag{1}$$

where ω_1 and ω_2 are penalty coefficients developed in order to avoid geometries with high number of discretization elements within the unit cell and allowing, when using a three frequency points evaluation, individuals with larger bandwidth to prevail.

A full–wave simulation using Method of Moments is carried out on a single design, i.e. unit cell of the infinite periodic surface and individual of a set population. The starting point is a random initial population of individuals. The external parameters of the structure (i.e. substrate thickness and dielectric constant) are fixed, altogether with the periodicity of the planar EBG. The geometry of the aperture is subject to the GP optimization, while the unit square cell within which each individual/design can evolve is fixed together with its discretization step.

The set of admissible solution is then composed by every geometry/aperture that can be designed in this square, built as series of segments that can evolve in every direction, with no limit on the number of segments, on their width and length and number of subsequent ramifications. We have fixed the discretization step within the unit cell in order to pose a limit not only to the computational burden but also to the geometrical spatial bandwidth of the possible solutions. In such a way we obtain a stabilizing effect on the problem, as much as shown in (Collin, 1985) for a different problem, namely wire antennas.

The phase of the reflection coefficient, computed at one or more frequencies depending on the goal, is then incorporated into the GP strategy for the evaluation procedure, the fitness function determining the environment within which the solutions "live" and the best

individual of a generation is selected. The evolutionary operators (reproduction, crossover and mutation) are then applied to the best individual leading to the subsequent evolution of the population and the next generation. In this way the geometrical properties are optimized to evolve the best solution (zero phase at the desired resonant frequency).

3. Single and multi–layer EBG full–wave analysis

Various techniques have been proposed in literature in order to analyze frequency selective surfaces (FSS) (Bardi et al., 2002; Bozzi & Perregrini, 1999; Harms et al., 1994; Mittra et al., 1988; Wu, 1995). The standard method of moments (MoM) approach is based on the induced electric currents on the FSS but it can be prohibitively costly from a computational point of view, if not even impractical in some cases, and this could explain why MoM is so unpopular.

Frequency Selective Surfaces (FSS) consist of two-dimensional periodic arrays of metallic patches patterned on a dielectric substrate or apertures etched on a metal screen, either entities can be isolated or connected in a rectangular grid. Hence, for any FSS, we can consider either the periodicity of the metallic patches or that of the apertures. By taking properly into account the continuity of electric or magnetic currents along adjacent cells we can conveniently adopt one of the two approaches, considering as unknowns of the problem either the electric or magnetic currents.
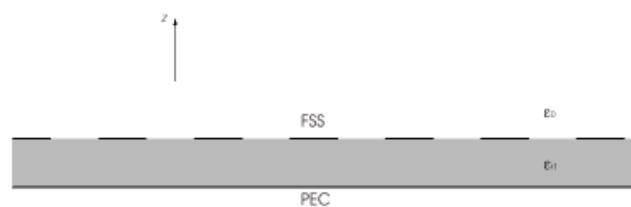

Fig. 6. Cross section view of a single layer FSS with dielectric substrate on ground plane.

The integral equation for the electric field (EFIE) applied to the periodic array of metal patches and the integral equation for the magnetic field (MFIE) applied to the periodic array of apertures thus represent two alternative formulations of the same problem, yielding to the same solution. The corresponding equivalent circuit for each approach is shown in Fig.8

Using a MoM approach based on the apertures, a very effective procedure can be devised (Deias & Mazzarella, 2006).

The aperture oriented approach (i.e. MFIE formulation) starts by applying the equivalence theorem (Balanis, 1996). The aperture is closed by a conductive sheet, and two unknown magnetic current densities $\mathbf{M}_A$ and $-\mathbf{M}_A$ on the opposite sides of the conductive sheet, as shown in Fig.7, are defined so that the continuity of the tangential electric field is guaranteed.

The MoM matrix is then obtained by imposing the continuity of the tangential component of the magnetic field across the aperture. The magnetic field is computed using a Green function in the spectral domain, too. But the relevant equivalent circuit, shown in Fig.8(b), allows to decouple the two regions below and above the metallization. This is a key feature not available in the conventional method based on the EFIE: in Fig.8(a) we can see that the equivalent circuit in this case bounds together the different regions.
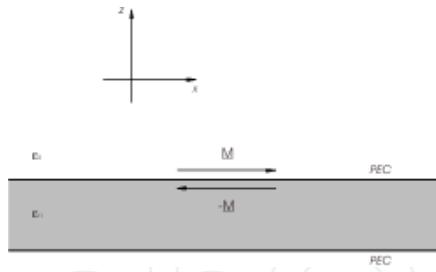
Fig. 7. Unit cell geometry of a Frequency Selective Surface with a dielectric substrate on ground plane, and magnetic currents equivalent to an aperture. The air–dielectric interface is a PEC.
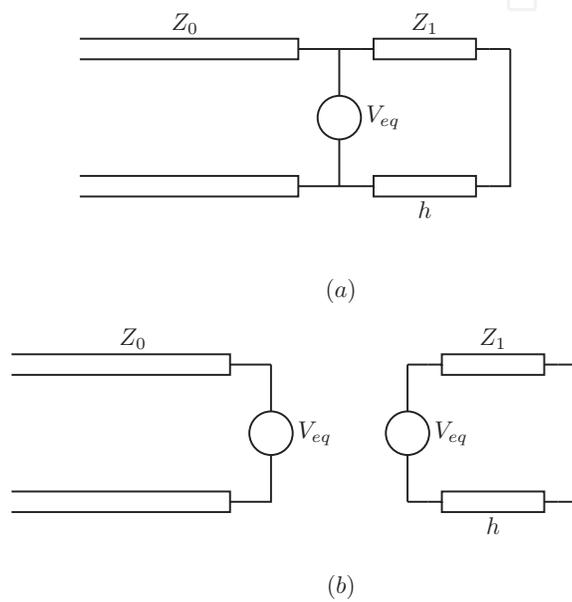

(a)

(b)

Fig. 8. Equivalent circuits resulting from the equivalence applied to a FSS (in the spectral domain): (a) metallic patches; (b) apertures.

As a consequence of our aperture approach, the MoM matrix can be decoupled in the sum of "localized" admittance matrices, each one relevant to a single region. For multi–layered FSS the advantages of the aperture approach are far more greater (Asole et al., 2007).

Let's consider the 3–layer AMC structure as shown in Fig.9, since it contains all the features of the method. The generalization to N-layer FSS is really straightforward.
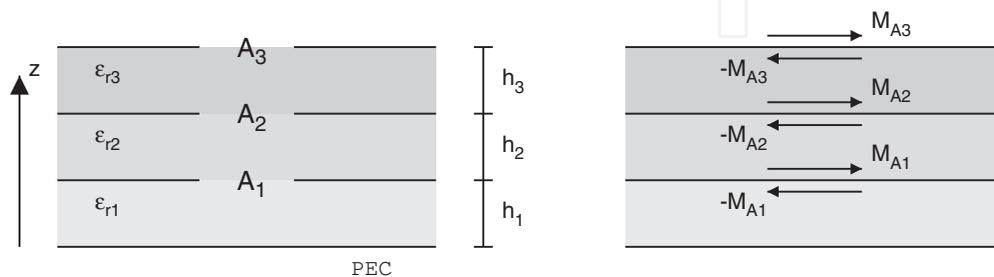

Fig. 9. Geometry of a 3–layer structure and magnetic currents equivalent to the apertures (central cell).

The dielectric layers can be chosen with the desired physical parameter and a superstrate can also be used to cover the structure. The unit cell of the periodic printed surfaces on the different layers may be of different shape but they must have the same periodicity.

According to the equivalence theorem, each aperture is closed by a PEC, and two unknown magnetic current densities $\mathbf{M}_{A_{nm}}$ and $-\mathbf{M}_{A_{nm}}$ on the opposite sides are defined in order to guarantee the continuity of the tangential electric field. By the Floquet theorem, the equivalent currents on the $(n, m)th$ cell of the periodic surface are connected to the central one by:

$$\mathbf{M}_{A,nm} = e^{-j\beta n d_x x} e^{-j\beta m d_y y} \mathbf{M}_A \tag{2}$$

where $\mathbf{M}_A$ is the current in the central cell.

As a consequence, only the current in the central cell is the unknown of the problem, and need to be discretized as a linear combination of N_b basis functions:

$$\mathbf{M}_A = \sum_{n=1}^{N_b} m_n^A \, \mathbf{f}_n \tag{3}$$

Then we obtain the MoM linear equation system by imposing the continuity of the tangential component of the magnetic field across each aperture. Again, by the Floquet theorem, this continuity needs to be forced only on the central cell (see Fig.**??**). It can be easily seen that, in the multilayered structure, we can distinguish three cases, namely an aperture lying on the first layer, on an intermediate layer or on the last layer.

For the first layer, i.e. for the discontinuity A_1, the continuity of the transverse magnetic field can be written as:

$$\mathbf{H}_{1,t}^{A_1 A_1} = \mathbf{H}_{2,t}^{A_1 A_1} + \mathbf{H}_{2,t}^{A_2 A_1} \tag{4}$$

which is then enforced in a *weak* form. A set of testing functions is selected and the boundary condition on the magnetic field is multiplied by each testing function and the result integrated over aperture. Choosing the Galerkin method, i.e. the testing functions used are the same basis functions used to express the unknown magnetic currents, we obtain for layer A_1:

$$\int_{A_1} \mathbf{H}_{1,t}^{A_1 A_1} \cdot \mathbf{f}_m = \int_{A_1} \mathbf{H}_{2,t}^{A_1 A_1} \cdot \mathbf{f}_m + \int_{A_1} \mathbf{H}_{2,t}^{A_2 A_1} \cdot \mathbf{f}_m, \qquad m = 1, \ldots, N_b \tag{5}$$

which, introducing the Green Functions can be written as:

$$\int_{A_1} \langle \hat{\mathbf{G}}_1^{A_1 A_1}, -\mathbf{M}_{A_1} \rangle \cdot \mathbf{f}_m = \int_{A_1} \langle \hat{\mathbf{G}}_2^{A_1 A_1}, \mathbf{M}_{A_1} \rangle \cdot \mathbf{f}_m +$$
$$\int_{A_1} \langle \hat{\mathbf{G}}_2^{A_2 A_1}, \mathbf{M}_{A_2} \rangle \cdot \mathbf{f}_m, + \int_{A_1} \langle \hat{\mathbf{G}}_2^{A_2 A_1}, \mathbf{M}_{A_2} \rangle \cdot \mathbf{f}_m, \qquad m = 1, \ldots, N_b \tag{6}$$

Expressing the unknown magnetic currents in the form (3):

$$\sum_{n=1}^{N_b} -m_n^{A_1} \left(\int_{A_1} \left(\int_{A_1} \hat{\mathbf{G}}_1^{A_1 A_1} \cdot \hat{\mathbf{f}}_n^{A_1} \right) \cdot \mathbf{f}_m^{A_1} + \int_{A_1} \left(\int_{A_1} \hat{\mathbf{G}}_2^{A_1 A_1} \cdot \hat{\mathbf{f}}_n^{A_1} \right) \cdot \mathbf{f}_m^{A_1} \right)$$
$$= \sum_{n=1}^{N_b} m_n^{A_2} \int_{A_1} \left(\int_{A_1} \hat{\mathbf{G}}_2^{A_2 A_1} \cdot \hat{\mathbf{f}}_n^{A_2} \right) \cdot \mathbf{f}_m^{A_1}, \qquad m = 1, \ldots, N_b \tag{7}$$

where the l.h.s. term represents the self–term, i.e. the effect of the magnetic current $\mathbf{M}_{A_1}$ on the aperture A_1, and the r.h.s. term is the coupling term, i.e. the effect of the magnetic current $\mathbf{M}_{A_2}$ on the aperture A_1.

For the second discontinuity A_2, as for any intermediate aperture, enforcing the boundary condition we obtain:

$$\mathbf{H}_{2,t}^{A_2 A_2} + \mathbf{H}_{2,t}^{A_1 A_2} = \mathbf{H}_{3,t}^{A_2 A_2} + \mathbf{H}_{3,t}^{A_3 A_2} \tag{8}$$

which leads to:

$$\sum_{n=1}^{N_b} -m_n^{A_2} \left(\int_{A_2} \left(\int_{A_2} \hat{\mathbf{G}}_2^{A_2 A_2} \cdot \hat{\mathbf{f}}_n^{A_2} \right) \cdot \mathbf{f}_m^{A_2} + \int_{A_2} \left(\int_{A_2} \hat{\mathbf{G}}_3^{A_2 A_2} \cdot \hat{\mathbf{f}}_n^{A_2} \right) \cdot \mathbf{f}_m^{A_2} \right) =$$

$$\sum_{n=1}^{N_b} m_n^{A_3} \int_{A_2} \left(\int_{A_2} \hat{\mathbf{G}}_3^{A_3 A_2} \cdot \hat{\mathbf{f}}_n^{A_3} \right) \cdot \mathbf{f}_m^{A_2} - \sum_{n=1}^{N_b} m_n^{A_1} \int_{A_2} \left(\int_{A_2} \hat{\mathbf{G}}_2^{A_1 A_2} \cdot \hat{\mathbf{f}}_n^{A_1} \right) \cdot \mathbf{f}_m^{A_2} \tag{9}$$

where $m = 1, \ldots, N_b$ and the l.h.s. term represents the self–term and the r.h.s. term the coupling terms, i.e. the effect of the magnetic currents $\mathbf{M}_{A_3}$ and $\mathbf{M}_{A_1}$ on the aperture A_2.

For the last (third) discontinuity A_3, the boundary condition leads to:

$$\mathbf{H}_{3,t}^{A_3 A_3} + \mathbf{H}_{3,t}^{A_2 A_3} = \mathbf{H}_{4,t}^{A_3 A_3} + \mathbf{H}_{inc,t} \tag{10}$$

and we obtain:

$$\sum_{n=1}^{N_b} -m_n^{A_3} \left(\int_{A_3} \left(\int_{A_3} \hat{\mathbf{G}}_3^{A_3 A_3} \cdot \hat{\mathbf{f}}_n^{A_3} \right) \cdot \mathbf{f}_m^{A_3} + \int_{A_3} \left(\int_{A_3} \hat{\mathbf{G}}_4^{A_3 A_3} \cdot \hat{\mathbf{f}}_n^{A_3} \right) \cdot \mathbf{f}_m^{A_3} \right)$$

$$= -\sum_{n=1}^{N_b} m_n^{A_2} \int_{A_3} \left(\int_{A_3} \hat{\mathbf{G}}_3^{A_2 A_3} \cdot \hat{\mathbf{f}}_n^{A_2} \right) \cdot \mathbf{f}_m^{A_3} - \int_S \mathbf{H}_{inc} \cdot \mathbf{f}_m^{A_3}(x,y) \, dS \tag{11}$$

where $m = 1, \ldots, N_b$ and, on the l.h.s we have the self–term and the first r.h.s. term is the coupling term, i.e. the effect of the magnetic current $\mathbf{M}_{A_2}$ on the aperture A_3. The second term of the r.h.s represent the known terms of the MoM system.

The presence of the coupling terms is the critical point in the multi–layer formulation. The key feature of the aperture approach, as previously illustrated, relies on the decoupling of the different regions. If we have a more general structure made up of N layers, we know that when dealing with the aperture A_1, which lies in the bottom layer, we only have to consider the effect of the magnetic current on the aperture A_2. When considering the aperture A_N, the last one, we only have to consider the effect of the magnetic current on the aperture A_{N-1}, and when considering any intermediate aperture A_i, for $i = 2, ..., N-1$ we have to take into account only the effect of the apertures immediately below and above, i.e. A_{i-1} and A_{i+1}. Equations (7),(9),(11) can be written in matrix form:

$$\mathcal{Y} \cdot \mathcal{M} = \mathcal{T} \tag{12}$$

where $\mathcal{Y}$ is the coefficient matrix, $\mathcal{M}$ is the vector of the unknown coefficients, i.e. the magnetic current on the apertures, and $\mathcal{T}$ is the r.h.s, which represent the incident magnetic field on the last aperture A_3.

The solution of the above equation (12) yields the unknown induced magnetic current on the apertures. The reflection coefficient is then easily calculated from the magnetic current on the upper layer.

It is important to stress out that inserting more layers will result in a larger matrix, affecting thus the overall computational time, yet for each additional layer only two blocks have to be computed.

The explicit evaluation of MoM system matrix $\mathcal{Y}$ requires the computation of the magnetic fields we previously introduced in (6),(8),(10). These are total magnetic fields,i.e. fields due to the magnetic currents of all the periodicity cells. Since the problem is linear, we start computing the magnetic field due to the magnetic current of a single cell. This field can be expressed in terms of a spectral domain (dyadic) Green function $\hat{\mathbf{G}}(u,v)$ connecting the transverse magnetic current density on the aperture to the transverse magnetic field:

$$\mathbf{H}_t^{unit\ cell}(x,y) = \int_{-\infty}^{+\infty} \int_{-\infty}^{+\infty} \hat{\mathbf{G}}(u,v) \cdot \hat{\mathbf{M}}(u,v)\ e^{-j(ux+vy)}\ du\,dv \tag{13}$$

where $\mathbf{M}$ is the magnetic current on the aperture of the central cell.

We can then write the overall magnetic transverse field of the infinite planar array by summing (13) on the infinite cells of the AMC:

$$\mathbf{H}_t(x,y) = \sum_r \sum_s e^{-jk_0 r d_x \sin\theta \cos\phi}\ e^{-jk_0 s d_y \sin\theta \sin\phi}\ .$$

$$\cdot \int_{-\infty}^{+\infty} \int_{-\infty}^{+\infty} \hat{\mathbf{G}}(u,v) \cdot \hat{\mathbf{M}}(u,v)\ e^{-j(ux+vy)}\ du\,dv \tag{14}$$

where d_x and d_y are the periodicity along the x–axis and the y–axis respectively, (θ, ϕ) is the direction of the incident field and k_0 is the free–space propagation constant.

Equation (14) can be simplyfied taking into account the periodicity of the structure. The fields on either side of the AMC can be expanded in terms of the Floquet space harmonics (Munk, 2000). Therefore the cell summation in (14) can be rearranged (Pozar & Schaubert, 1984) using the Poisson formula. As a result, we obtain the following compact expression:

$$\mathbf{H}_t(x,y) = \frac{4\pi^2}{d_x d_y} \sum_r \sum_s \hat{\mathbf{G}}(u_r,v_s) \cdot \hat{\mathbf{M}}(u_r,v_s)\ e^{-j(u_r x+v_s y)} \tag{15}$$

where the summation is now on the Floquet modes.

Equation (15) can be used for both fields (above and below the metallization) by using the pertinent Green function, which can be derived from the equivalent circuit shown in Fig.8(b) and setting $\mathbf{M} = \pm\mathbf{M}_A$ (current on the pertinent layer of the central cell).

4. Single–layer EBG design results

Significative and promising results have been found when this approach was applied to a single–layer EBG structure (Deias et al., 2009a).

One of the most interesting structures that can be found in literature is the Itoh's UC–EBG structure (Yang et al., 1999), shown in Fig.10(a) consisting of a Jerusalem cross aperture.

The reference structure has periodicity $d_x = d_y = 3.048mm$, $h = 0.635mm$ and $\varepsilon = 10.2$, displaying a resonant frequency at 14.25GHz. The reflection coefficient is shown in Fig.10(b).

We decided to use these parameters as constraints for our test, in order to compare the results obtained using the GP approach with Itoh's UC–EBG.

We used for the full–wave analysis of the periodic structure our previously developed Fortran code, implementing the aperture approach described in the previous section. Furthermore
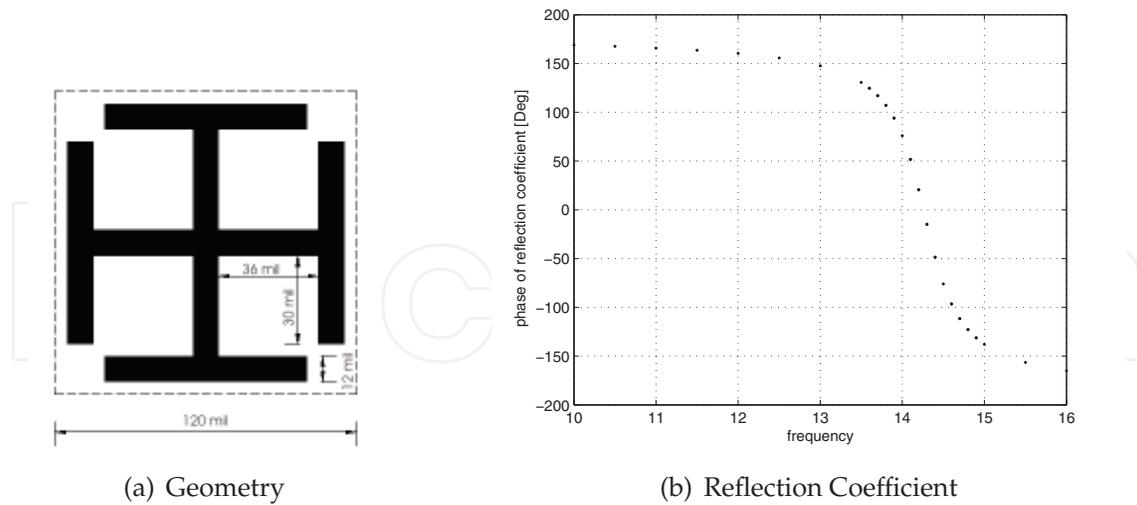
(a) Geometry

(b) Reflection Coefficient

Fig. 10. UC–EBG

this approach is irrespective of the particular shape of the metallization, which in the GP optimization stage cannot be known in advance.

The GP optimization was launched to find the best structure, keeping as fixed parameters the periodicity, substrate dielectric constant and thickness, as shown in the following table.

Fixed Parameters	
Center Frequency	14.2 GHz
Periodicity (unit square cell)	$d_x = 3.048$ mm; $d_y = 3.048$ mm
Substrate dielectric constant	$\epsilon_r = 10.2$
Substrate thickness	0.635 mm
Discretization step	0.1016 mm $(30 \times 30 \ grid)$

Table 1. Data

In Fig.11 and Fig.12 we can see two different runs of our optimization. And in Tab.2 it is shown how the goal is achieved, in comparison also to the reference structure.

	Phase of Refl. Coeff.		
	14 GHz	14.2 GHz	14.4 GHz
Itoh (lit.)	76.05°	20.52°	-48.56°
Case A	57.8°	2.2°	-63.16°
Case B	39.28°	0.83°	-35.16°
Case C	13.06°	-6.13°	-24.93°

Table 2. Results

In Case A we used for the unit cell a discretization step of 0.1016mm, making the playground for the GP optimization a 30x30 grid. The penalty coefficients, both for the number of unknowns (i.e. borders of the discretized geometry) and for the bandwidth were initially not too strict, making the evolution process quickly evolve towards quite bulky structures. The resonant frequency was reached after few generations (for case A at gen. 13 the phase of the reflection coefficient is 2.2°).
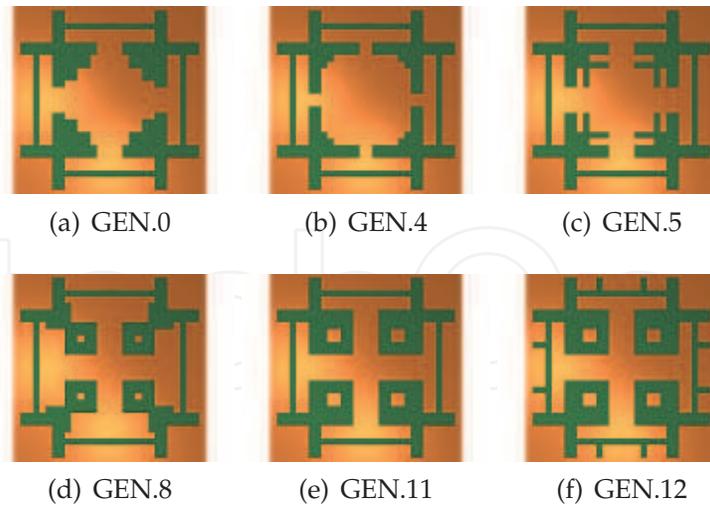
| (a) GEN.0 | (b) GEN.4 | (c) GEN.5 |
| (d) GEN.8 | (e) GEN.11 | (f) GEN.12 |

Fig. 11. Case A.

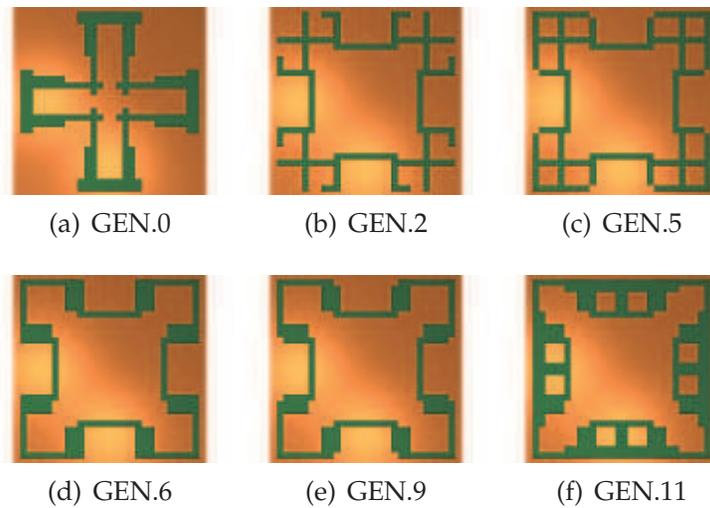| (a) GEN.0 | (b) GEN.2 | (c) GEN.5 |
| (d) GEN.6 | (e) GEN.9 | (f) GEN.11 |

Fig. 12. Case B.

In Case B we then acted more stringently on the penalty coefficients. The structure remains spatially more limited, as the number of unknowns is kept reasonably low, and the bandwidth is largely improved. The number of generations in order to achieve a good result is still low.

As expected, the geometries resemble the reference one and other well–known configurations, since the only stringent requirement in this case is the resonant frequency. The fitness in this case is relatively simple, aimed almost uniquely to direct the evolution process towards a structure that resonates at the desired frequency. We then can insert an additional penalty coefficient in order to maximize the bandwidth, a secondary objective overlapped to the main goal.

Finally, as we can see in Fig.14(c), we allowed the geometry to touch the borders of the unit cell, thus considering a continuous aperture (while the geometry of the metallic patch will therefore be finite), and we found out a further improvement in the bandwidth. In Fig.15 the entire surface is shown.
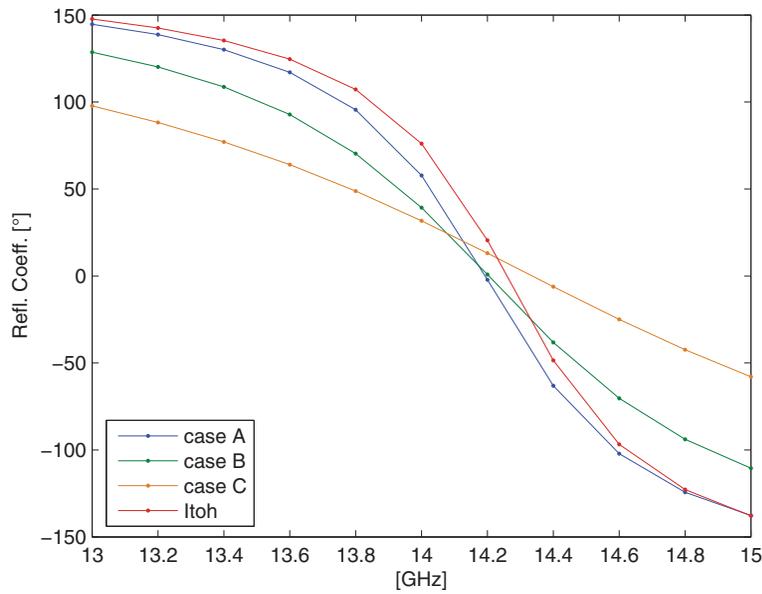
Fig. 13. Reflection Coefficient.

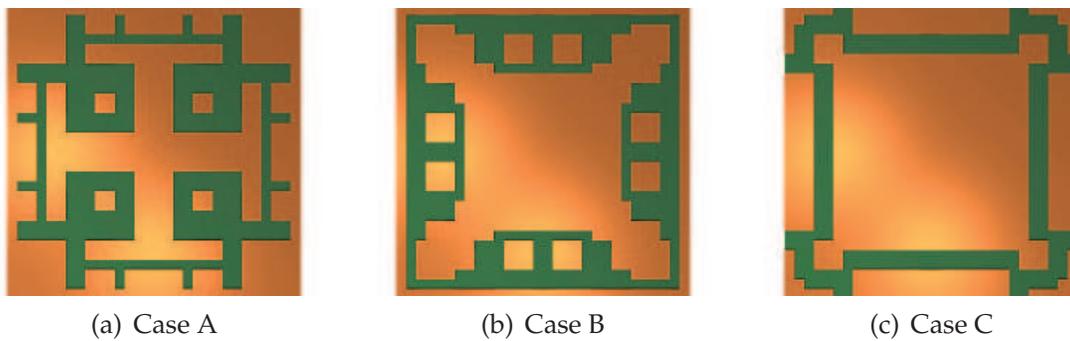(a) Case A   (b) Case B   (c) Case C

Fig. 14. Best individual

We can exploit this approach using a more complex fitness function in order to obtain, for example, larger bandwidth (Deias et al., 2009a),as shown in case B, or at more interesting frequencies (Deias et al., 2010).

It is well known that there is a growing interest in antennas integrated with EBG surfaces for communication system applications, covering the 2.45 GHz and the 5 GHz wireless networking bands (Hung-Hsuan et al., 2007; Zhu & Langley, 2009). As proof of the effectiveness of our approach a simple EBG surface at this working frequencies was found with a yet limited computational effort.

Fixed parameters in this case are the following:

In Fig.16(b) we can see the reflection coefficient for the best individual shown Fig.16(a), as obtained after nine generations. The performance of our optimization is quite good leading to a simple and effective solution with a yet limited computational effort.

These results prove that the main advantage of the genetic approach is to be identified in the generalization of the "solution space", evolution being able to breed geometries that we could
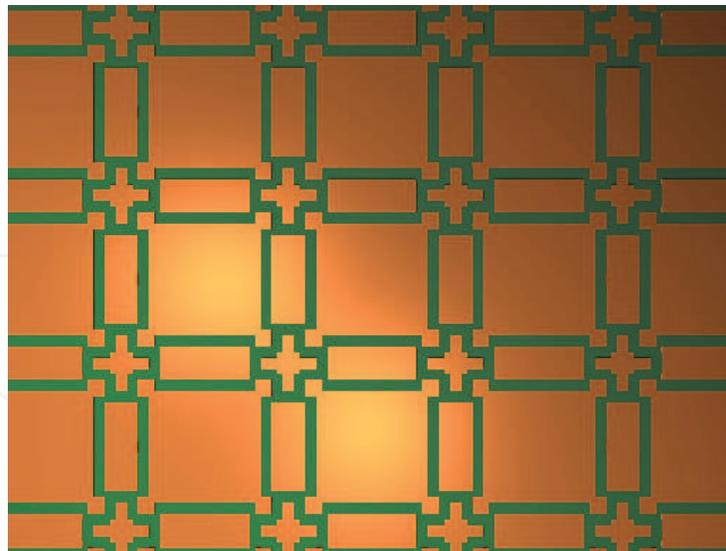
Fig. 15. EBG Surface (Case C)

Fixed Parameters	
Center Frequency	2.45 GHz
Periodicity (unit square cell)	$d_x = 40$ mm; $d_y = 40$ mm
Substrate dielectric constant	$\epsilon_r = 1.38$
Substrate thickness	2.2 mm
Discretization step	0.8 mm $(50 \times 50$ $grid)$

Table 3. Data

never think of. Evolutionary computation on the other hand let us scope through geometries as though they were human–described.

5. Multi–layer EBG design results

The periodic surfaces in the single–layer configuration shown so far exhibit perfect reflection or transmission only at resonance. However, many applications, exploiting the filtering properties of frequency selective surfaces, seek for a resonant curve with a flat top and faster roll off. This goal can be achieved by using two or more periodic surfaces cascaded with dielectric slabs sandwiched in between . By using multiple layers of frequency selective surfaces as part of the substrate we operate in a manner similar to that used for designing broad–band microwave filters. With such a configuration typically we can obtain a bandwidth that is considerably larger than that of a single structure.

Genetic Programming strategy in conjunction with the flexible aperture approach previously described proved to be effective in the design and optimization of EBG surfaces in the case of a two–layer structure with the same geometry in both layers. When considering more layers or different geometries we only have to take into consideration an increased computational effort.

In the case of a two–layer configuration with the following fixed parameters:

We obtained the following geometry after two generations, each generation with a population of 150 individuals:
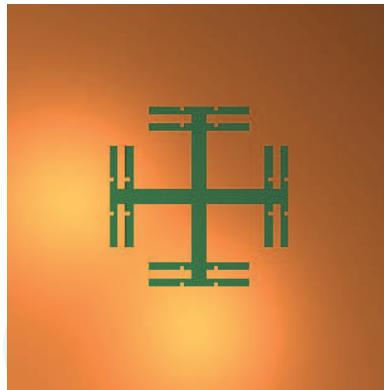
(a) Geometry
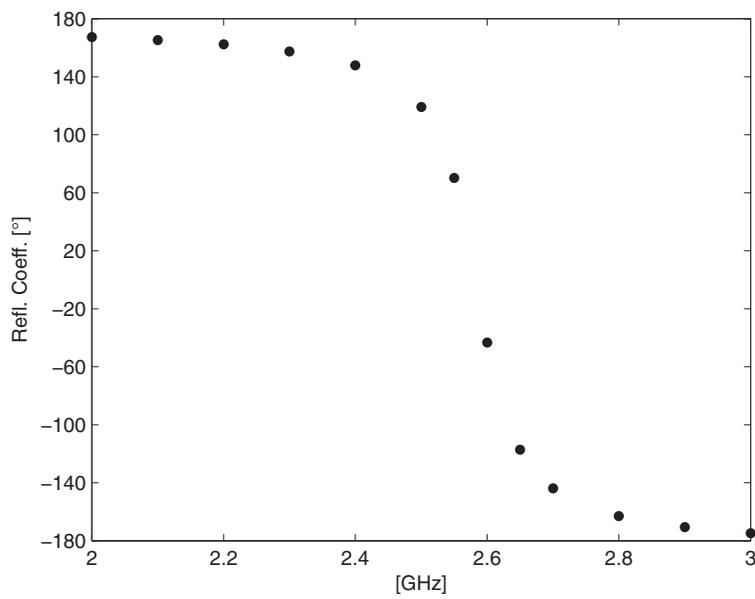
(b) Reflection Coefficient

Fig. 16

Fixed Parameters	
Center Frequency	2.45 GHz
Periodicity (unit square cell)	$d_x = 3.048$ mm; $d_y = 3.048$ mm
Substrate dielectric constant	$\epsilon_r = 10.2$
Substrate thickness	3.354772 mm
Discretization step	0.1524 mm $(20 \times 20 \ grid)$

Table 4. Data

This quite simple result proves that genetic programming can be efficiently adopted for this kind of design synthesis and optimization even in the case of complex structures consisting of multiple layers of EBG surfaces. Moreover the fitness function can be modified in order to take into consideration other requirements.
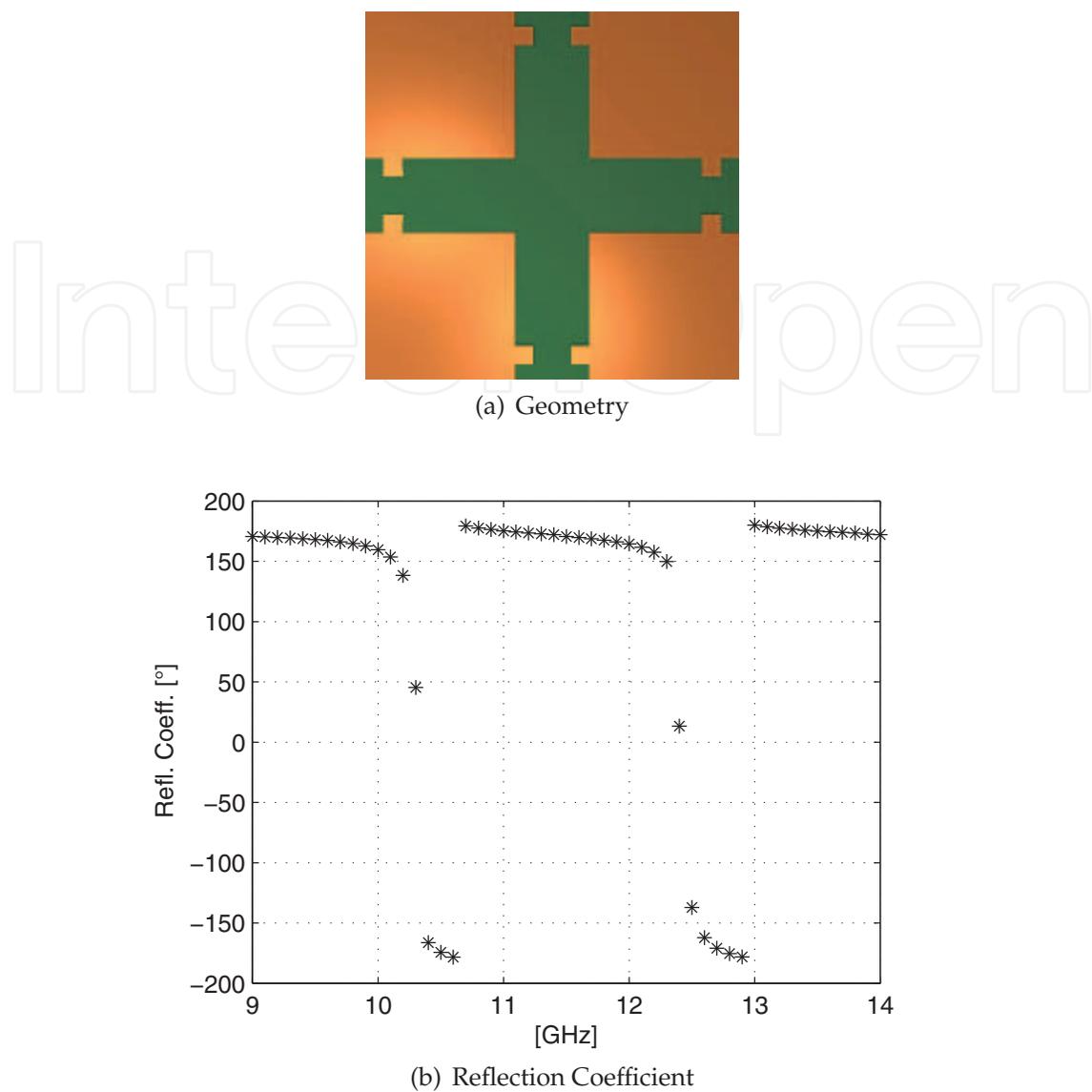
(a) Geometry

(b) Reflection Coefficient

Fig. 17

6. Acknowledgements

7. References

Asole, F., Deias, L. & Mazzarella, G. (2007). A flexible full–wave analysis of multilayered amc using an aperture oriented approach, *J. Electrom. Waves Appl.* 21(No. 14): 2059–2072.

Balanis, C. A. (1996). *Antenna Theory – Analysis and Design*, Wiley, New York.

Bardi, I., Remski, R., Perry, D. & Cendes, Z. (2002). Plane wave scattering from frequency–selective surfaces by the finite element method, *IEEE Trans. Magn.* 38(No 2): 641–644.

Bozzi, M. & Perregrini, L. (1999). Efficient analysis of thin conductive screens perforated periodically with arbitrarily shaped apertures, *IEE Electronics Letters* 35(No 13): 1085–1087.

Bray, M., Bayraktar, Z. & Werner, D. (2006). Ga optimized ultra–thin tunable ebg amc surfaces, *IEEE Antennas and Propagation Society International Symposium* pp. 410 – 413.

Collin, R. E. (1985). *Antennas and Radiowave Propagation*, McGraw–Hill.

Deias, L. & Mazzarella, G. (2006). Aperture oriented approach to the analysis of artificial magnetic conductors and first–order circuit model validation, *12th International Symposium on Antenna Technology and Applied Electromagnetics (ANTEM) and Canadian Radio Sciences (URSI/CNC)*.

Deias, L., Mazzarella, G. & Sirena, N. (2009a). Bandwidth optimization of ebg surfaces using genetic programming, *LAPC 2009. Antennas and Propagation Conference.* pp. 593–596.

Deias, L., Mazzarella, G. & Sirena, N. (2009b). Synthesis of ebg surfaces using evolutionary optimization algorithms, *EuCAP 2009. 3rd European Conference on Antennas and Propagation.* pp. 99 –102.

Deias, L., Mazzarella, G. & Sirena, N. (2010). Ebg substrate synthesis for 2.45 ghz applications using genetic programming, *IEEE Antennas and Propagation Society International Symposium (APSURSI)* pp. 1–4.

Feresidis, A. P., Goussetis, G., Wang, S., & Vardaxoglou, J. C. (2005). Artificial magnetic conductor surfaces and their application to low–profile high–gain planar antennas, *IEEE Trans. Antennas Propagat.* Vol. 53(No. 11): 209–215.

Fogel, D. (2006). *Evolutionary Computation: Toward a New Philosophy of Machine Intelligence*, IEEE Press, New York.

Ge, Y., Esselle, K. & Hao, Y. (2007). Design of low–profile high-gain ebg resonator antennas using a genetic algorithm, *IEEE Antennas and Wireless Propagation Letters* 6: 480 – 483.

Gonzalo, R., de Maagt, P. & Sorolla, M. (1999). Enhanced patch-antenna performance by suppressing surface waves using photonic-bandgap substrates, *IEEE Trans. Microw. Theory Tech.* Vol. 47(No. 11): 2131–2138.

Harms, P., Mittra, R. & Wae, K. (1994). Implementation of the periodic boundary condition in the finite–difference time–domain algorithm for fss structures, *IEEE Trans. Antennas Propagat.* 42: 1317–1324.

Hosseini, M., Pirhadi, A. & Hakkak, M. (2006). Design of a novel amc with little sensitivity to the angle of incidence and very compact size, *IEEE Antennas and Propagation Society International Symposium*.

Hung-Hsuan, L., Chun-Yih, w. & Shih-Huang, Y. (2007). Metamaterial enhanced high gain antenna for wimax application, *TENCON*.

Jones, E. A. & Joines, W. T. (2000). Evolutionary optimization of yagi–uda antennas, *Antennas and Propagation Magazine* 42(No. 3).

Kovács, P., Raida, Z. & Lukes, Z. (2010). Design and optimization of periodic structures for simultaneous ebg and amc operation, *COMITE 15th International Conference on Microwave Technique* pp. 195 – 198.

Koza, J. R. (1992). *Genetic Programming: On the Programming of Computers by Means of Natural Selection*, Mit Press.

Lohn, J. D., Kraus, W. F., Linden, D. S. & Colombano, S. (2001). Evolutionary optimization of yagi–uda antennas, *Proceedings of the 4th International Conference on Evolvable Systems: From Biology to Hardware* pp. 236–243.

Michalewicz, Z. (1992). *Genetic Algorithms + Data Structures = Evolution Programs*, Springer-Verlag.

Mittra, R., Chan, C. & Cwik, Y. (1988). Techniques for analyzing frequency selective surfaces – a review, *Proceedings IEEE*, pp. 1593–1615.

Munk, B. (2000). *Frequency Selective Surfaces: Theory and Design*, Wiley Interscience, New York.

Pozar, D. M. & Schaubert, D. H. (1984). Scan blindness in infinite phased arrays of printed dipoles, *IEEE Trans. Antennas Propagat.* 32(No. 6): 602–610.

Sievenpiper, D., Zhang, L., Broas, R., Alexopolou, N. & Yablonovitch, E. (1999). High-impedance electromagnetic surfaces with a forbidden frequency band, *IEEE Trans. Microw. Theory Tech.* Vol. 47(No. 11): 2059–2074.

Tavallaee, A. & Rahmat-Samii, Y. (2007). A novel strategy for broadband and miniaturized ebg designs: hybrid mtl theory and pso algorithm, *IEEE Antennas and Propagation Society International Symposium* pp. 161 – 164.

Wu, T. K. (1995). *Frequency Selective Surface and Grid Array*, Wiley, New York.

Yang, F. R., Ma, K. P., Quian, Y. & Itoh, T. (1999). A novel tem waveguide using uniplanar compact photonic-bandgap (uc-pbg)structure, *IEEE Trans. Microw. Theory Tech.* Vol. 47(No. 11): 2092–2098.

Yeo, J., Mittra, R. & Chakravarty, S. (2002). A ga–based design of electromagnetic bandgap (ebg) structures utilizing frequency selective surfaces for bandwidth enhancement of microstrip antennas, *IEEE Antennas and Propagation Society International Symposium* 2: 400 – 403.

Zhu, S. & Langley, R. (2009). Dual-band wearable textile antenna on an ebg substrate, *IEEE Trans. Antennas Propagat.* Vol. 57(No. 4): 926–935.
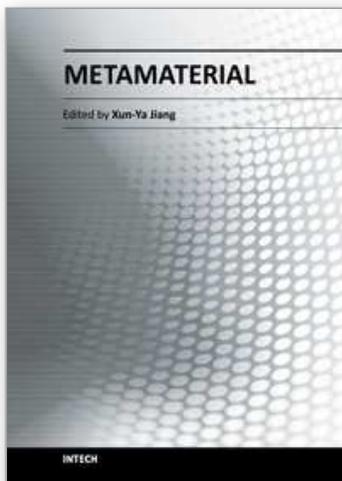
Metamaterial

Edited by Dr. Xun-Ya Jiang

ISBN 978-953-51-0591-6

Hard cover, 620 pages

Publisher InTech

Published online 16, May, 2012

Published in print edition May, 2012

In-depth analysis of the theory, properties and description of the most potential technological applications of metamaterials for the realization of novel devices such as subwavelength lenses, invisibility cloaks, dipole and reflector antennas, high frequency telecommunications, new designs of bandpass filters, absorbers and concentrators of EM waves etc. In order to create a new devices it is necessary to know the main electrodynamical characteristics of metamaterial structures on the basis of which the device is supposed to be created. The electromagnetic wave scattering surfaces built with metamaterials are primarily based on the ability of metamaterials to control the surrounded electromagnetic fields by varying their permeability and permittivity characteristics. The book covers some solutions for microwave wavelength scales as well as exploitation of nanoscale EM wavelength such as visible specter using recent advances of nanotechnology, for instance in the field of nanowires, nanopolymers, carbon nanotubes and graphene. Metamaterial is suitable for scholars from extremely large scientific domain and therefore given to engineers, scientists, graduates and other interested professionals from photonics to nanoscience and from material science to antenna engineering as a comprehensive reference on this artificial materials of tomorrow.

How to reference

In order to correctly reference this scholarly work, feel free to copy and paste the following:

Luisa Deias, Giuseppe Mazzarella and Nicola Sirena (2012). Synthesis of Planar EBG Structures Based on Genetic Programming, Metamaterial, Dr. Xun-Ya Jiang (Ed.), ISBN: 978-953-51-0591-6, InTech, Available from: http://www.intechopen.com/books/metamaterial/synthesis-of-planar-ebg-structures-based-on-evolutionary-programming

INTECH
open science | open minds